Appendix A

Single-pole Miller Compensation: A First-order Analysis

The generic two-stage voltage gain block with minor-loop compensation (**fig. 1**) is modelled in **figure A1** by a differential voltage controlled current source (VCCS) driving a TIS consisting of a current controlled current source (CCCS) and load resistor $\mathbf{R_{eq}}$, which is the means by which the TIS's output current is expressed as a voltage.

Resistor $\mathbf{R_{eq}}$ represents the modulus of the effective impedance at the output of the TIS, and comprises the parallel combination of the TIS's output impedance and the output buffer's input impedance. The TIS's current gain $\beta_{eq.}$ is merely the product of the current gains of transistors **T5** and **T6**.

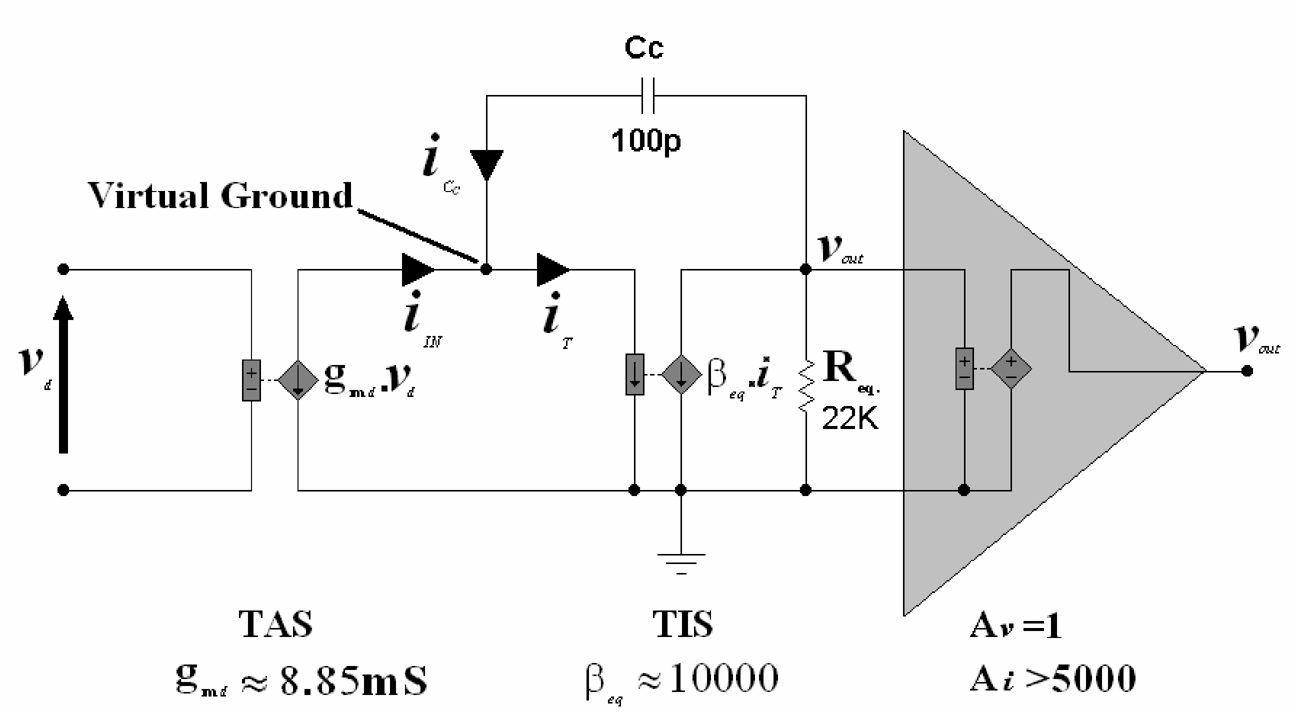

Figure A1. First-order model of the single-pole compensated voltage gain block.

It is assumed here that the minor feedback loop defined by $\mathbf{C_C}$ is stable, and that the amplifier's unity-gain frequency f_U is sufficiently low so that non-dominant poles have negligible effect on its open-loop transfer function.

At DC the TIS, comprising **T5** and **T6** in **figure A1**, possesses a low input resistance compared to the TAS's output resistance. As local feedback through $\mathbf{C_C}$ increases beyond the dominant pole frequency, the TIS's input impedance rapidly tends to zero; the TIS's input is then virtually at ground potential, and the entire output voltage may be deemed to appear across $\mathbf{C_C}$.

Invoking Kirchoff's current Law with respect to the output node (**fig. A1**)

$$-i_{C_C} - \beta_{eq} i_T + \frac{(0 - v_{out})}{R_{eq}} = 0$$

$\Rightarrow$

$$i_{C_C} + \beta_{eq} i_T + \frac{v_{out}}{R_{eq}} = 0 \qquad (1a)$$

Similarly at the input node

$$i_{in} + i_{C_C} - i_T = 0 \qquad (2a)$$

Since shunt-applied negative feedback makes the TIS's input node a virtual ground at the frequencies of interest, then

$$i_{Cc} = sC_C v_{out} \qquad (3a)$$

Substituting **(3a)** into **(1a)**

$$sC_C v_{out} + \beta_{eq} i_T + \frac{v_{out}}{R_{eq}} = 0 \qquad (4a)$$

Substituting **(3a)** into **(2a)**

$$i_{in} + sC_C v_{out} - i_T = 0 \qquad (5a)$$

Equation **(5a)** is multiplied by β_{eq} as a prelude to eliminating i_T :

$$i_{in}\beta_{eq} + sC_C v_{out}\beta_{eq} - \beta_{eq} i_T = 0 \qquad (6a)$$

Thus, adding equation **(4a)** to **(6a)** eliminates i_T :

$$i_{in}\beta_{eq} + sC_C v_{out}\beta_{eq} + sC_C v_{out} + \frac{v_{out}}{R_{eq}} = 0 \qquad (7a)$$

$\Rightarrow$

$$\frac{v_{out}}{i_{in}}(s) = -\frac{\beta_{eq} R_{eq}}{1 + sC_C R_{eq}(\beta_{eq} + 1)}$$

Since $(\beta_{eq} >> 1)$, then it may be assumed with negligible error that $(\beta_{eq} + 1) \approx \beta_{eq}$, and

$$\frac{v_{out}}{i_{in}}(s) \approx \frac{-\beta_{eq} R_{eq}}{1 + sC_C R_{eq}\beta_{eq}} \qquad (8a)$$

First stage transconductance $\mathbf{g_{md}}$ in **figure A1** (with degeneration resistors $\mathbf{R_{e1}}$ and $\mathbf{R_{e2}}$) is given by $\mathbf{g_{md}} \approx (\mathbf{r_e} + \mathbf{R_{e1}})^{-1}$.

The intrinsic emitter resistance $\mathbf{r_e}$ in each TAS transistor is merely the reciprocal of the stage's undegenerated transconductance $\mathbf{g_{mo}}$, *viz.* $\mathbf{r_e} \approx 1/\mathbf{g_{mo}}$, and $\mathbf{g_{mo}} \approx \mathbf{qI_C/KT} = \mathbf{I_C/V_T}$.

Where $\mathbf{K}$ is Boltzmann's constant ($\sim 1.38 \times 10^{-23}$ joules/Kelvin), $\mathbf{T}$ the absolute temperature, (Kelvin), $\mathbf{q}$ the electronic charge ($\sim 1.6 \times 10^{-19}$ coulomb) and $\mathbf{V_T}$ the thermal voltage (~ 26mV at room temperature).

Thus, at room temperature, and with the component values in **figure A1**, $\mathbf{g_{md}} \approx \left[(38.5 \times 2\mathbf{mA})^{-1} + 100\Omega\right]^{-1} \approx 8.85\mathbf{mS}$.

But

$$\boldsymbol{i_{IN}} = -\boldsymbol{g_{md} v_d}$$

Thus, the amplifier's forward path gain is given by

$$\frac{\boldsymbol{v_{out}}}{\boldsymbol{v_d}}(\boldsymbol{s}) \approx \frac{\boldsymbol{g_{md}}\beta_{\boldsymbol{eq}}\boldsymbol{R_{eq}}}{1 + \boldsymbol{sC_C}\beta_{\boldsymbol{eq}}\boldsymbol{R_{eq}}} \tag{9a}$$

or

$$\frac{\boldsymbol{v_{out}}}{\boldsymbol{v_d}}(\boldsymbol{s}) \approx \boldsymbol{K} \cdot \frac{1}{1 + \boldsymbol{sC_C}\beta_{\boldsymbol{eq}}\boldsymbol{R_{eq}}} \tag{10a}$$

Where **K** is the forward path gain at DC:

$$\boldsymbol{K} = \boldsymbol{g_{md}}\beta_{\boldsymbol{eq}}\boldsymbol{R_{eq}} \tag{11a}$$

From **(10a)** the dominant pole frequency $\boldsymbol{f_D}$ is given by

$$\boldsymbol{f_D} \approx \frac{1}{2\pi \boldsymbol{C_C}\beta_{\boldsymbol{eq}}\boldsymbol{R_{eq}}} \tag{12a}$$

Unity-gain frequency $\boldsymbol{f_U}$ is obtained by merely equating **(9a)** to unity:

$$1 = \frac{\boldsymbol{g_{md}}\beta_{\boldsymbol{eq}}\boldsymbol{R_{eq}}}{1 + \omega_{\boldsymbol{U}}\boldsymbol{C_C}\beta_{\boldsymbol{eq}}\boldsymbol{R_{eq}}} \tag{13a}$$

$\Rightarrow$

$$f_U \approx \frac{\left(g_{md}\beta_{eq}R_{eq} - 1\right)}{2\pi C_C \beta_{eq} R_{eq}} \tag{14a}$$

In practice, only forward path gain well beyond the dominant pole frequency is of interest and, with respect to **equation (9a)**, the condition $\left(\beta_{eq}R_{eq} \to \infty\right)$ is invoked, so that

$$\left.\frac{v_{out}}{v_d}(s)\right|_{(10 f_D \le f \le f_U)} \approx \frac{g_{md}}{sC_C} \tag{15a}$$

Equation (14a) becomes

$$f_U \approx \frac{g_{md}}{2\pi C_C} \tag{16a}$$

Equation (15a) is valid only at frequencies well beyond the dominant pole. This is demonstrated by the plot of **figure A2** using typical values (**fig. A1**); the finite gain of the TIS introduces significant error at DC and infrasonic frequencies.

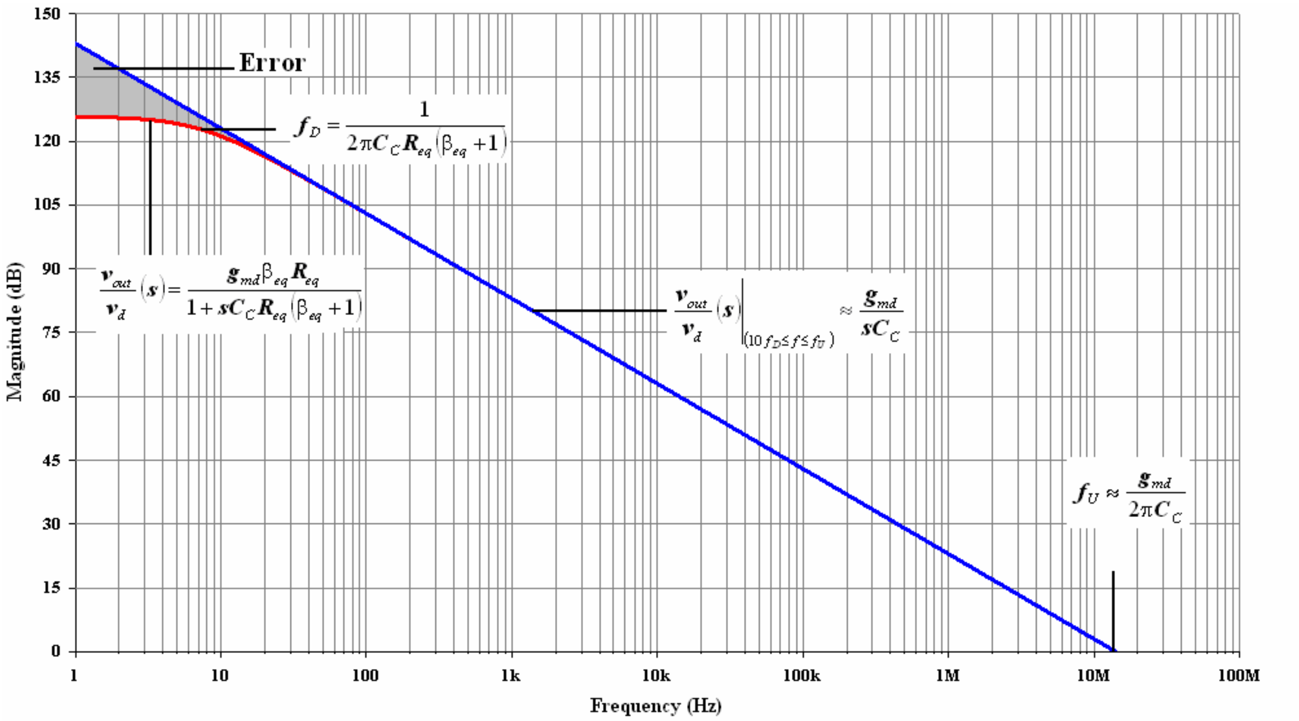

Figure A2. The simplification $\left(\beta_{eq}R_{eq} \to \infty\right)$ gives negligible error in the forward-path transfer function at the frequencies of interest.

Pole Splitting

The presence of the first non-dominant pole may be accommodated by performing a second order analysis in which the TIS is more accurately modelled by a voltage controlled current source (VCCS) with finite input and output shunt impedances[53,54], which give rise to two dominant poles (**fig. A3**). Capacitors $\mathbf{C_{eq1}}$ and $\mathbf{C_{eq2}}$ represent the equivalent shunt capacitance at the input and output nodes of the TIS, while the effective shunt resistance is represented by $\mathbf{R_{eq1}}$ and $\mathbf{R_{eq2}}$ respectively.

Tedious but rudimentary nodal analysis at the input and output of the TIS demonstrates that single-pole feedback compensation causes the first two dominant system poles to move apart, while the finite input voltage v_i generates a so-called feedforward current i_f through $\mathbf{C_C}$. Ultimately, the forward current gives rise to a non-minimum phase (RHP) zero when $\mathbf{C_C}$ short-circuits the TIS's load, $\mathbf{R_{eq2}} \,//\, 1/\mathbf{sC_{eq2}}$, so that $i_f = g_{m1} \cdot v_i$ and $v_{out} = 0$.

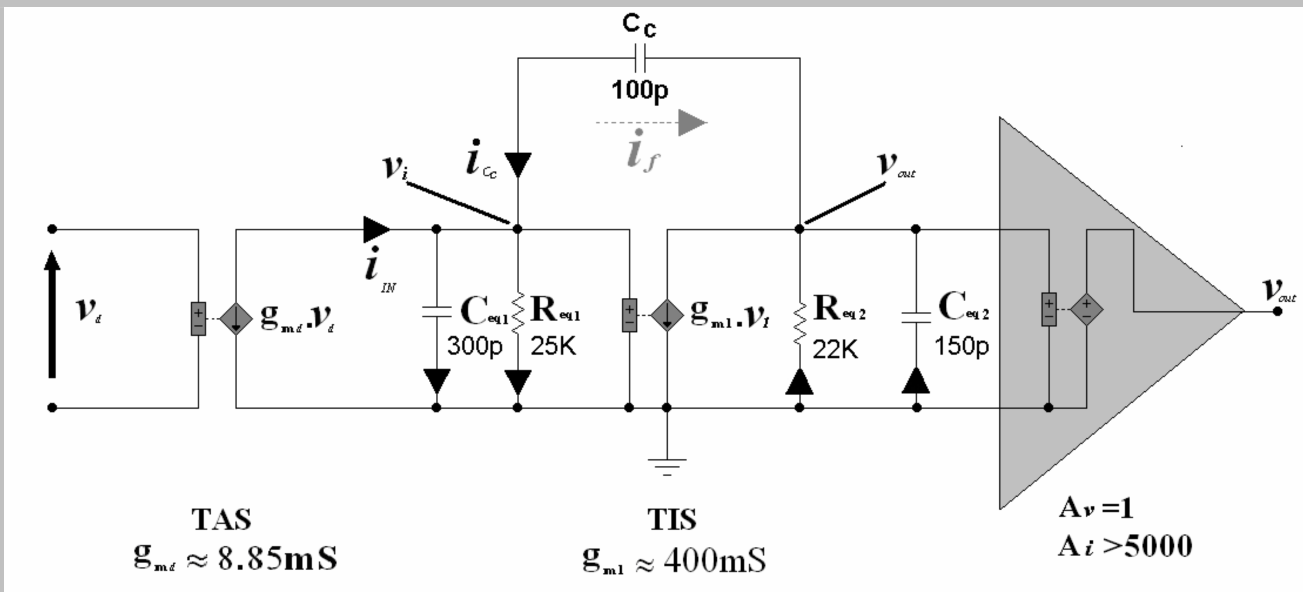

Figure A3. Second-order model of the single-pole compensated generic voltage gain block.

At the TIS's input node

$$-g_{md}.v_d - v_i.sC_C + v_{out}.sC_C - v_i.sC_{eq1} - v_i/R_{eq1} = 0 \tag{17a}$$

And at the TIS's output node

$$v_i.sC_C - v_{out}.sC_C - g_{m1}.v_i - v_{out}.sC_{eq2} - v_{out}/R_{eq2} = 0 \tag{18a}$$

Solving **(18a)** for v_i and substituting the result into **(17a)** eliminates v_i:

$$\frac{v_{out}}{v_d}(s) = \frac{g_{md}g_{m1}R_{eq1}R_{eq2}(1 - sC_C/g_{m1})}{s^2R_{eq1}R_{eq2}(C_CC_{eq2} + C_CC_{eq1} + C_{eq1}C_{eq2}) + s\{R_{eq1}(C_C + C_{eq1}) + R_{eq2}(C_C + C_{eq2}) + g_{m1}C_CR_{eq1}R_{eq2}\} + 1} \tag{19a}$$

or

$$\frac{v_{out}}{v_d}(s)=\frac{K\left(1-sC_C/g_{m1}\right)}{s^2R_{eq1}R_{eq2}\left(C_CC_{eq2}+C_CC_{eq1}+C_{eq1}C_{eq2}\right)+s\left\{R_{eq1}\left(C_C+C_{eq1}\right)+R_{eq2}\left(C_C+C_{eq2}\right)+g_{m1}C_CR_{eq1}R_{eq2}\right\}+1} \quad (20a)$$

Where K is the forward path gain at DC:

$$K=g_{md}g_{m1}R_{eq1}R_{eq2} \quad (21a)$$

From **equation (20a)**

$P_1\big|_{C_C=0}=-1/\left(R_{eq1}C_{eq1}\right)$ and $P_2\big|_{C_C=0}=-1/\left(R_{eq2}C_{eq2}\right)$.

The denominator in **(19a)** is a second order polynomial and provided $\mathbf{C_C} >> \mathbf{C_{eq1}} \vee \mathbf{C_{eq2}}$, the local loop is stable and assuming the poles are real it may be expressed as the product of two first-order factors:

$$Denominator(s)=\left(1+s/P_1\right)\left(1+s/P_2\right)=1+s\left(1/P_1+1/P_2\right)+s^2/\left(P_1P_2\right) \quad (22a)$$

By merely equating coefficients it is apparent that

$P_1\approx-1/\left(g_{m1}R_{eq1}R_{eq2}C_C\right)$, $P_2\approx-g_{m1}C_C/\left(C_{eq1}C_{eq2}+C_{eq1}C_c+C_{eq2}C_C\right)$ and $Z=g_{m1}/C_C$.

Where $\mathbf{P_1}$ is the dominant pole, $\mathbf{P_2}$ the first non-dominant pole and $\mathbf{Z}$ the right half plane zero.

Therefore, $\left|\mathbf{P_1}\right|\propto 1/\left(\mathbf{g_{m1}C_C}\right)$ and decreases as the product $\left(\mathbf{g_{m1}C_C}\right)$ increases, while $\left|\mathbf{P_2}\right|\propto\left(\mathbf{g_{m1}C_C}\right)$ and increases with increasing $\left(\mathbf{g_{m1}C_C}\right)$. Rough estimates of the variables $\mathbf{C_{eq1}}$, $\mathbf{C_{eq2}}$, $\mathbf{R_{eq1}}$ and $\mathbf{R_{eq2}}$ in (**fig. A3**) were obtained from a simplified hybrid-π (VCCS) BJT model, derived from **2N5551** datasheet characteristics, with $\mathbf{g_{m1}}$ modified to accommodate the current gain provided by emitter-follower **T6** (**fig. 1**). SPICE simulation of **figure A3** shows that $\mathbf{P_1}$ moves down from 21KHz, in the absence of $\mathbf{C_C}$, to 7Hz with $\mathbf{C_C}$ in-situ, while $\mathbf{P_2}$ moves from just 48KHz to over 70MHz (**fig. A4**).

The system therefore maintains a much wider bandwidth with dominant pole feedback compensation than would accrue if such a characteristic were realised by merely increasing shunt-capacitance at the input or output nodes of the TIS. This is unacceptable[28] as it adversely loads the TIS's collector, severely compromising second-stage linearity.

Moreover, dominant pole shunt compensation at either the TIS's input or output node would leave $\mathbf{P_2}$ virtually unchanged, and, consequently, the system's unity loop-gain bandwidth would necessarily have to be much less than 21KHz to guarantee stability when the major feedback loop is closed.

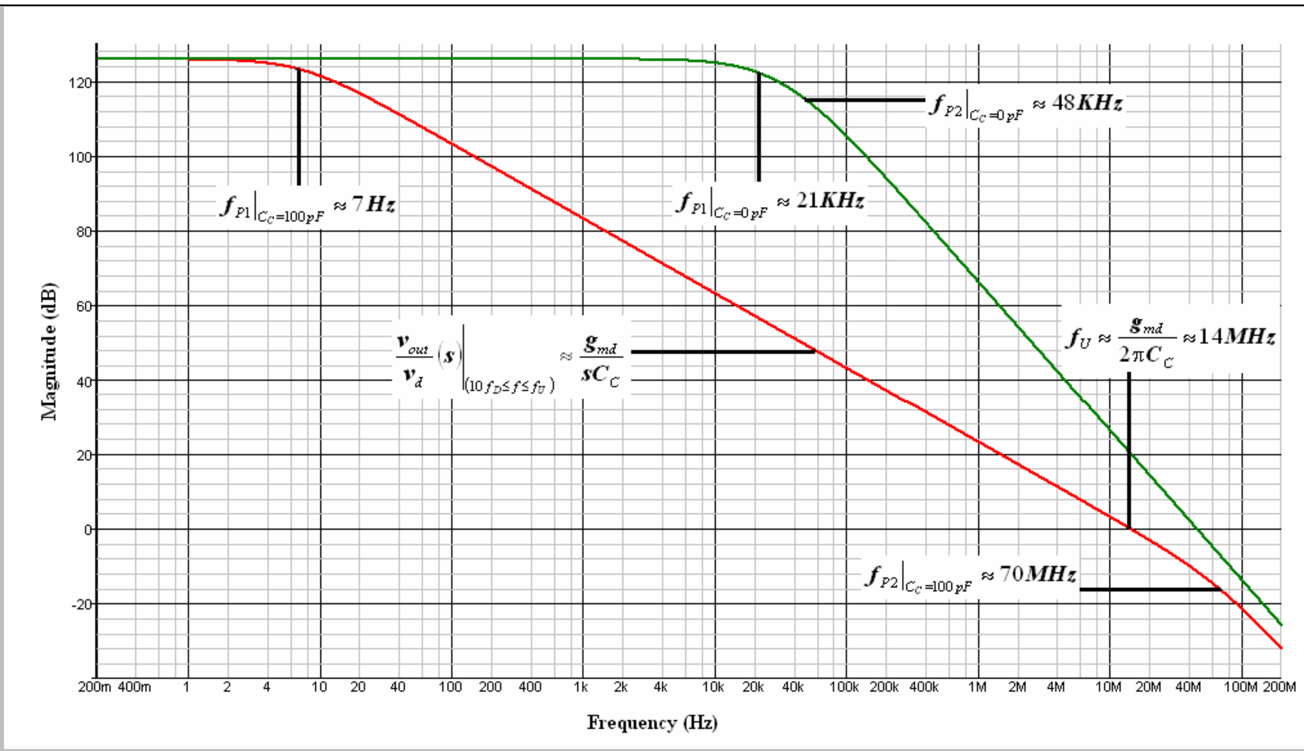

Figure A4. The apparent migration of dominant poles due to Miller-effect compensation on the forward path's frequency response (red trace). The green trace represents the uncompensated forward path's frequency response.

The RHP zero (not shown in **fig. A4**) has the magnitude response of an LHP zero (i.e. magnitude response 'breaks up') but the phase response of an LHP pole (i.e. phase response 'breaks down' or tends to -90 degrees in the limit) and might therefore be expected to compromise stability margins. This, however, is of no concern in discrete power amplifiers with an all-BJT second stage as $\mathbf{g_{m1}}$ is invariably much larger than $\mathbf{C_C}$ which ensures that the RHP zero resides well beyond the unity-gain bandwidth of the amplifier.

Determining system singularities in this fashion helps develop a vivid appreciation of circuit behaviour, but is only of academic interest to the designer of discrete amplifiers, as the solutions depend on imprecisely known variables such as $\mathbf{C_{eq1}}$ and $\mathbf{C_{eq2}}$ which, moreover, also vary dynamically.

In practice, the first-order approximation of **equation (16a)** is all that is required to determine the value of first stage transconductance and the corresponding size of compensation capacitor needed to ensure that non-dominant system singularities, including output stage poles, are relegated to well beyond the unity loop-gain frequency. For the practicing engineer, the design-stage analysis of second-order circuit behaviour is the province of SPICE simulators.